Glucan Binding Protein C of *Streptococcus mutans* Mediates both Sucrose-Independent and Sucrose-Dependent Adherence

Joshua Mieher, Matthew R. Larson, Norbert Schormann, Sangeetha Purushotham, Ren Wu, Kanagalaghatta R. Rajashankar, Hui Wu and Champion Deivanayagam

Supplemental Data Contents:

Supplemental Figures and Tables:

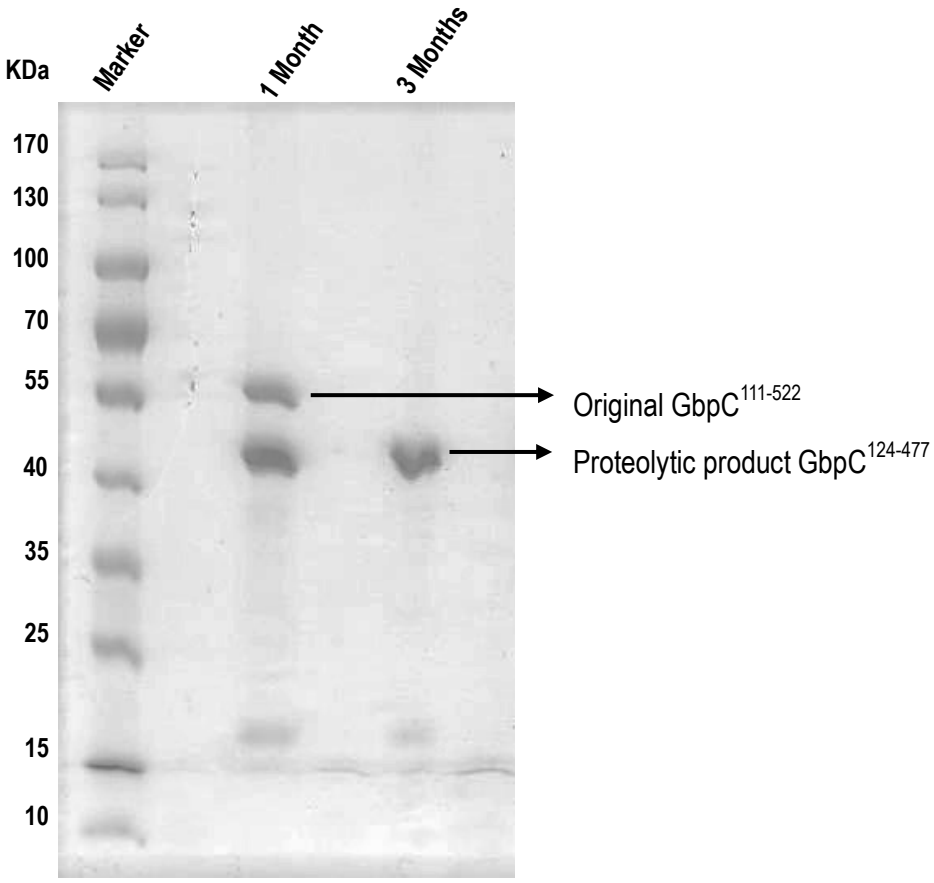

Supplemental Figure 1: SDS-PAGE gel shows the purified product within one and three months of purification. GbpC$^{111-522}$ undergoes proteolytic degradation and results in GbpC$^{124-477}$, whose crystal structure has now been resolved.

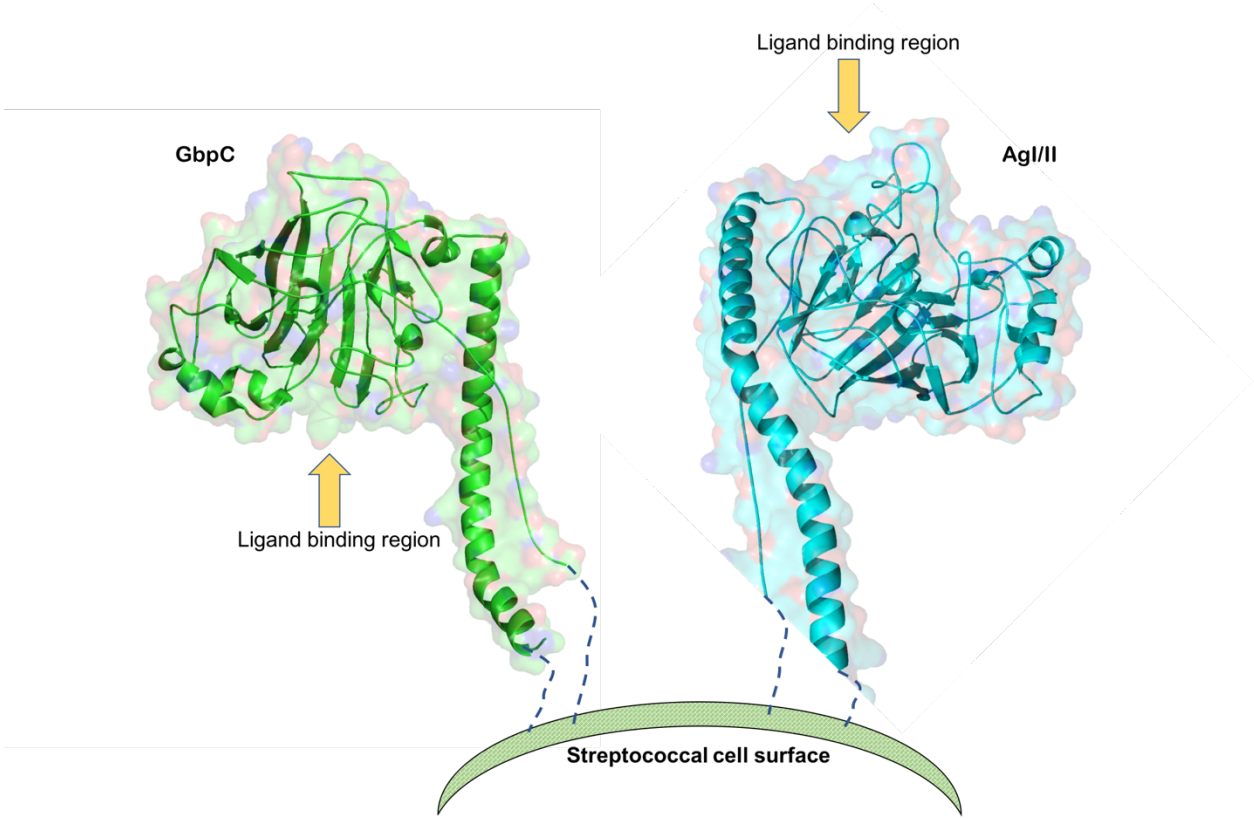

Supplemental Figure 2: These cartoons describe the orientation of the distant V-region of GbpC and AgI/II as it would appear based on the orientation of the helical region that anchors it to the cell surface. In this case, it is particularly interesting to note that the ligand binding regions of GbpC and AgI/II will be in opposite spatial orientation. This gives rise to the idea that while AgI/II could be thought of as the extended grabber of SAG/SRCR, the propensity for GbpC to bind to glucans (which are predominantly on the tooth surface) would serve to bring *S. mutans* closer to the surface, promoting colonization.

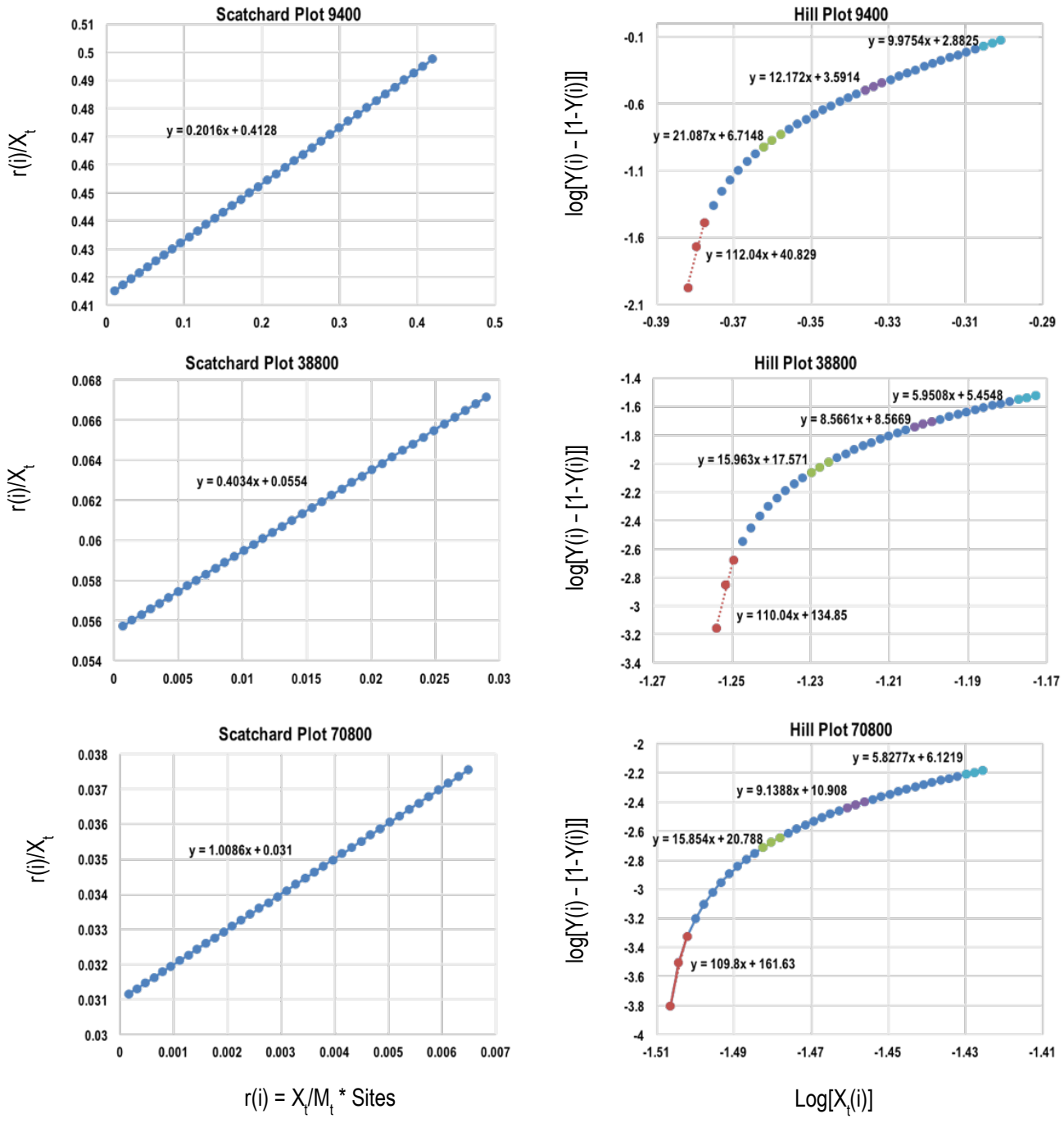

Supplemental Figure 3: Scatchard and Hill plots for 9400, 38800 and 70800 Da dextran. The linearity of the Scatchard plots describes a non-cooperative interaction that occurs between GbpC and dextran. In the Hill plot, the gradual reduction in the slopes indicates the saturation of the substrate over multiple injections, thereby describing the molecular model of interaction as shown in Figure 8.

A

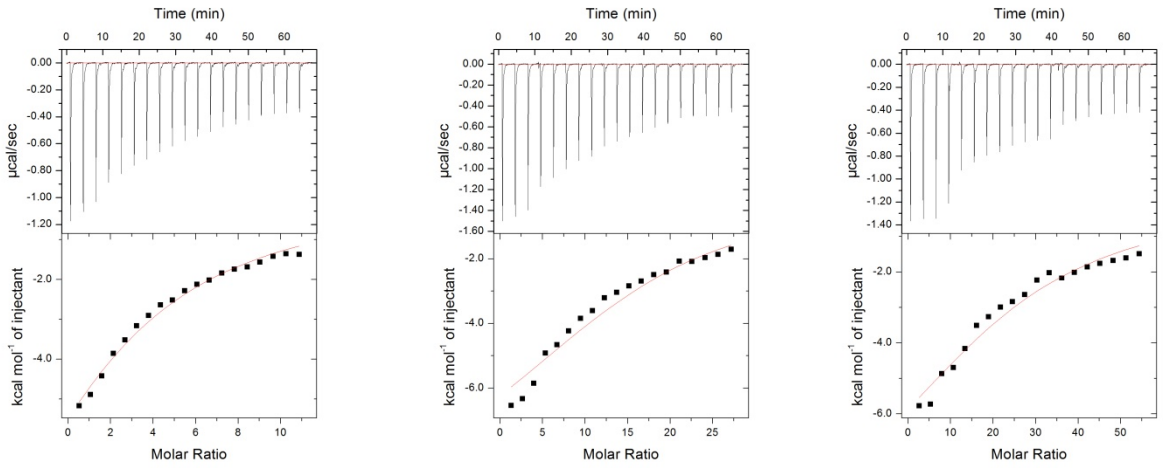

9400 Da Dextran **38800 Da Dextran** **70800 Da Dextran**

Tabulated results from reverse ITC experiments						
Syringe	**Cell**		***N***	***K_d*** (M)	***ΔH*** (cal/mol)	***ΔS*** (cal/mol/deg)
GbpC (mM)	**Dextran** (mM)	**Dextran** (Da)				
1.30	0.025	9400	3.55	$1.62 \pm 0.109 \times 10^{-4}$	$-1.495 +/- 0.05099 \times 10^{4}$	-32.8
1.30	0.010	38800	16.33	$8.93 \pm 2.47 \times 10^{-5}$	$-9.417 +/- 892.8 \times 10^{3}$	-13.1
1.30	0.005	70800	26	$1.02 \pm 0.18 \times 10^{-4}$	$-1.02 +/- 0.06994 \times 10^{4}$	-16

B

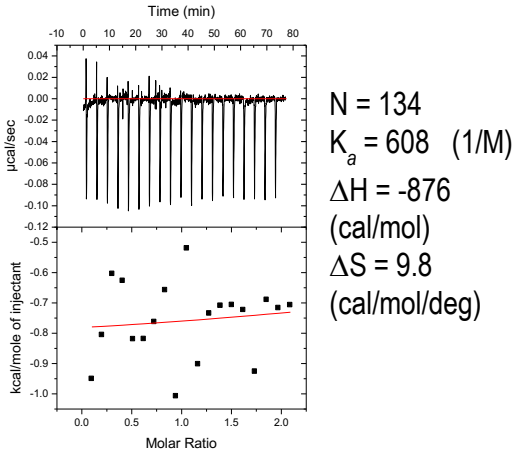

N = 134
K_a = 608 (1/M)
ΔH = -876 (cal/mol)
ΔS = 9.8 (cal/mol/deg)

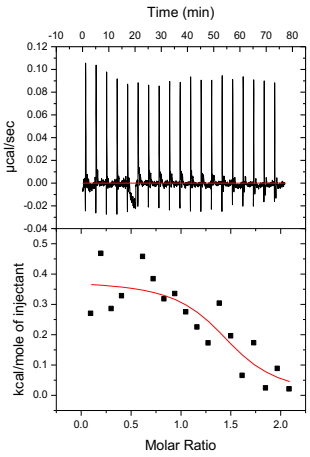

N= 1.46
K_a = 21400 (1/M)
ΔH = 378 (cal/mol)
ΔS = 25.7 (cal/mol/deg)

Supplemental Figure 4: *Panel A* shows preliminary reverse titration ITC experiments performed with GbpC in the syringe and dextran in the cell as opposed to those reported in figure 4. While auto fitting the thermograms in Origin 7.0, fixed N-values from previous experiments (Figure 4) were needed to achieve convergence. The affinity (K_d), enthalpy (ΔH) and entropy (ΔS) values are very similar to the experimental values reported in figure 4, thus confirming the nature of interactions that occur between GbpC and dextran. Unfortunately, better thermograms with higher 'C' values were not obtainable given the instrument limitations. *Panel B* contains ITC experiments to determine the interaction of AgI/II (left) and SspB (right) with dextran, indicating no specific adherence.

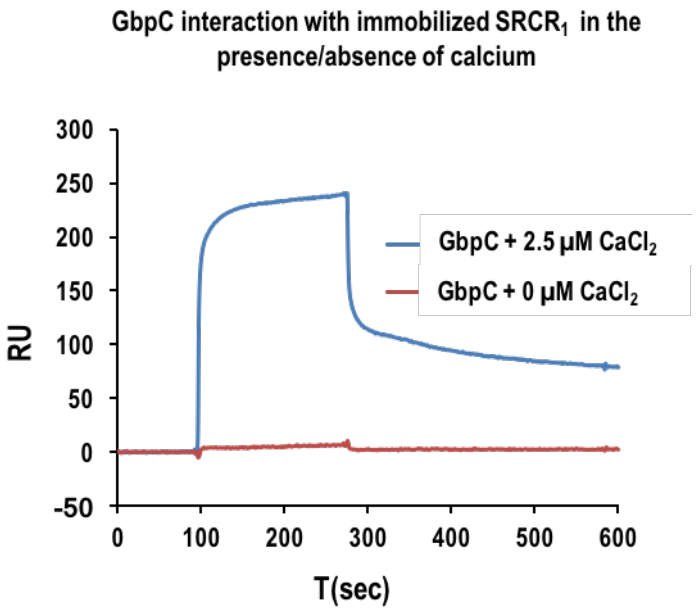

Supplemental Figure 5: SPR sensorgram for the interaction between GbpC and *i*SRCR$_1$ in the presence and absence of calcium. In the absence of calcium there is no interaction.

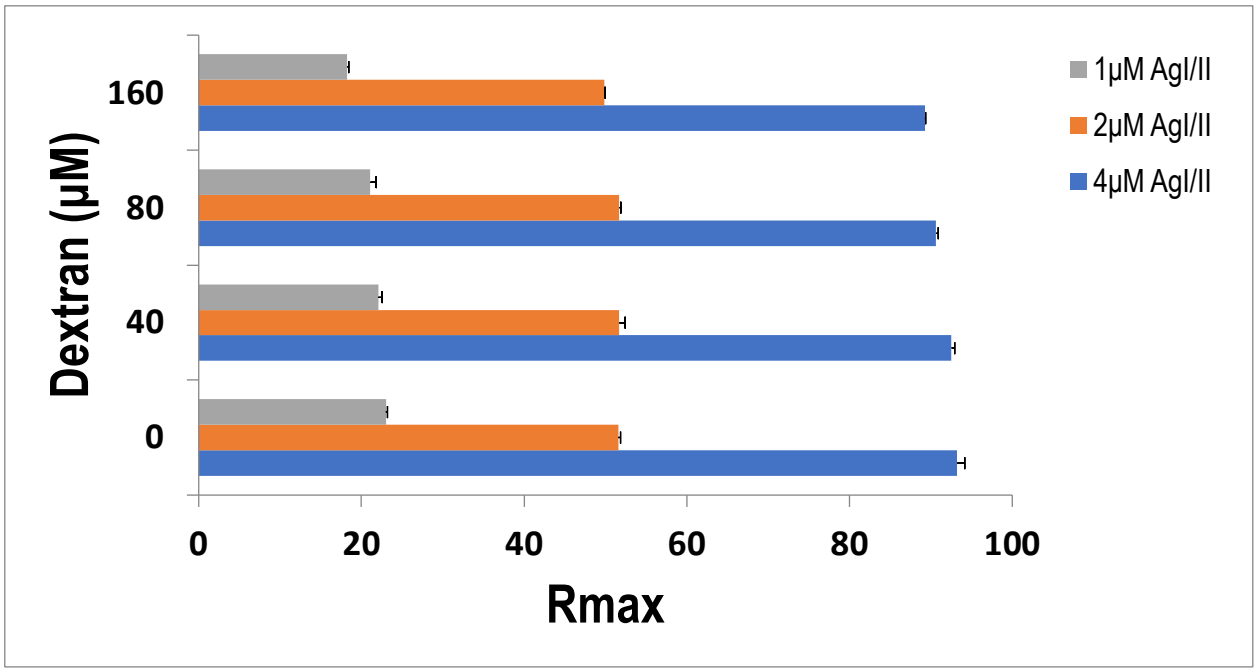

Supplemental Figure 6: The effect of 5000 Da Dextran on the adherence of AgI/II to immobilized $SRCR_1$ was evaluated in the presence of various concentrations of dextran. The result of the experiment shows that there is no change in the adherence characteristics of AgI/II to $SRCR_1$ in the presence of dextran, thus validating our ITC results, which demonstrates that AgI/II and SspB do not adhere to dextran. Similar values were seen for SspB (data not shown).

Calcium coordination bonds and distances									
GbpC-native structure					GbpC-BGC complex structure				
ID	Atom	Atom	Residue	Distance	ID	Atom	Atom	Residue	Distance
478 CA	CA	O	888 HOH	2.49	501 CA	CA	O3	601 BGC	2.33
478 CA	CA	O	347 SER	2.36	501 CA	CA	OE1	360 GLU	2.52
478 CA	CA	OE1	360 GLU	2.48	501 CA	CA	O2	601 BGC	2.38
478 CA	CA	O	524 HOH	2.38	501 CA	CA	OG	347 SER	2.32
478 CA	CA	OG	347 SER	2.45	501 CA	CA	O	347 SER	2.31
478 CA	CA	O	1014 HOH	2.47	501 CA	CA	OD1	349 ASN	2.31
478 CA	CA	OD1	349 ASN	2.31	501 CA	CA	O4	601 BGC	2.37
478 CA	CA	O	893 HOH	2.57	501 CA	CA	O	1 HOH	2.36

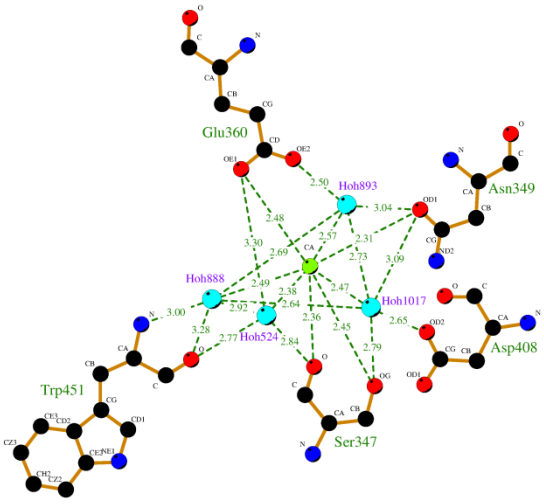

GbpC_native: Ca478 coordination

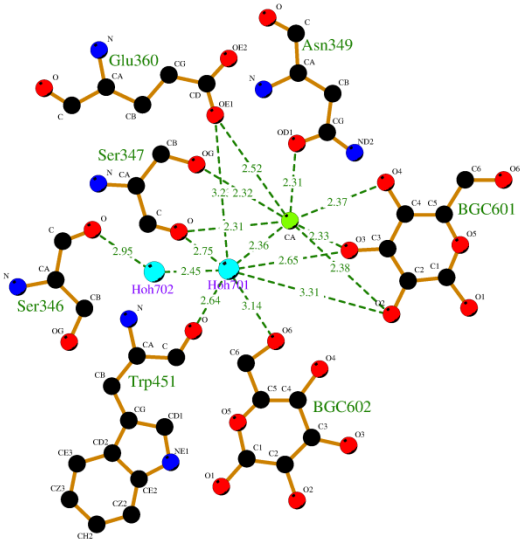

GbpC_BGC2: Ca501 coordination

Supplemental Figure 7: The table above and the two Ligplots below detail the interaction of the calcium atoms in the GbpC-native and the GbpC-BGC complex structures. Water molecules in the native structure are displaced to allow for the binding of the glucose molecule.

Table of hydrogen bonding distance with β-D-glucose				
ID	Atom	Atom	Residue	Distance
601 BGC	O1	O	449 THR	3.04
601 BGC	O1	OE2	360 GLU	3.37
601 BGC	O2	OE1	360 GLU	2.49
601 BGC	O2	OE2	360 GLU	2.36
601 BGC	O2	CA	501 CA	2.38
601 BGC	O2	O	1 HOH	3.31
601 BGC	O5	O	90 HOH	3.12
601 BGC	O4	OG	347 SER	2.25
601 BGC	O4	OD1	349 ASN	2.99
601 BGC	O4	OD1	408 ASP	3.17
601 BGC	O4	CA	501 CA	2.37
601 BGC	O4	OD2	408 ASP	2.45
601 BGC	O3	O	451 TRP	2.91
601 BGC	O3	N	451 TRP	3.26
601 BGC	O3	CA	501 CA	2.33
601 BGC	O3	O	1 HOH	2.65
601 BGC	O6	O	90 HOH	2.60
601 BGC	O6	ND2	349 ASN	3.27
601 BGC	O6	OD2	408 ASP	2.59
602 BGC	O2	O	414 GLY	2.78
602 BGC	O5	O	451 TRP	3.03
602 BGC	O4	O	17 HOH	2.61
602 BGC	O4	O	82 HOH	2.24
602 BGC	O3	O	107 HOH	2.92
602 BGC	O6	O	346 SER	2.28
602 BGC	O6	O	135 HOH	2.39

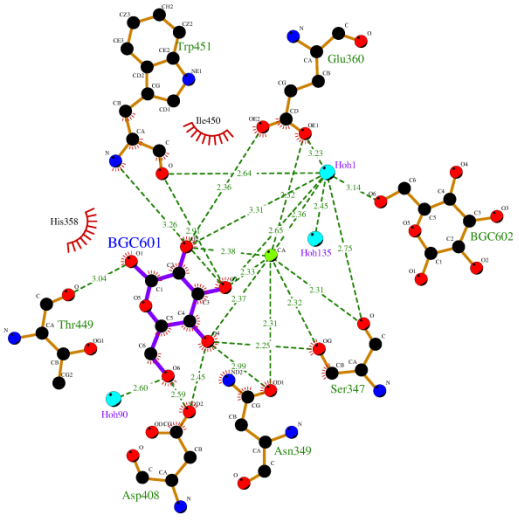

GbpC_BGC2: BGC601 hydrogen bonding

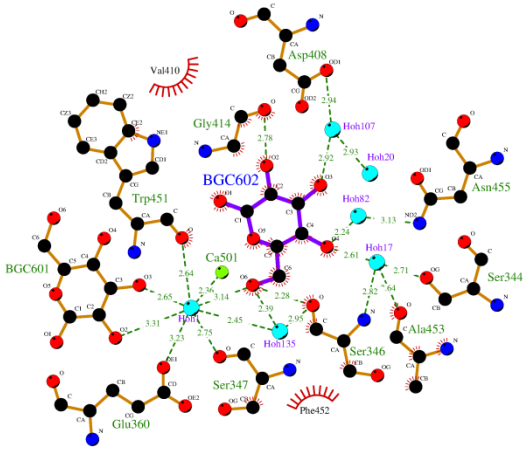

GbpC_BGC2: BGC602 hydrogen bonding

Supplemental Figure 8: The table above and the Ligplots below detail the interaction of the glucose molecules BGC1 and BGC2 in close proximity to the Ca^{2+} binding site.

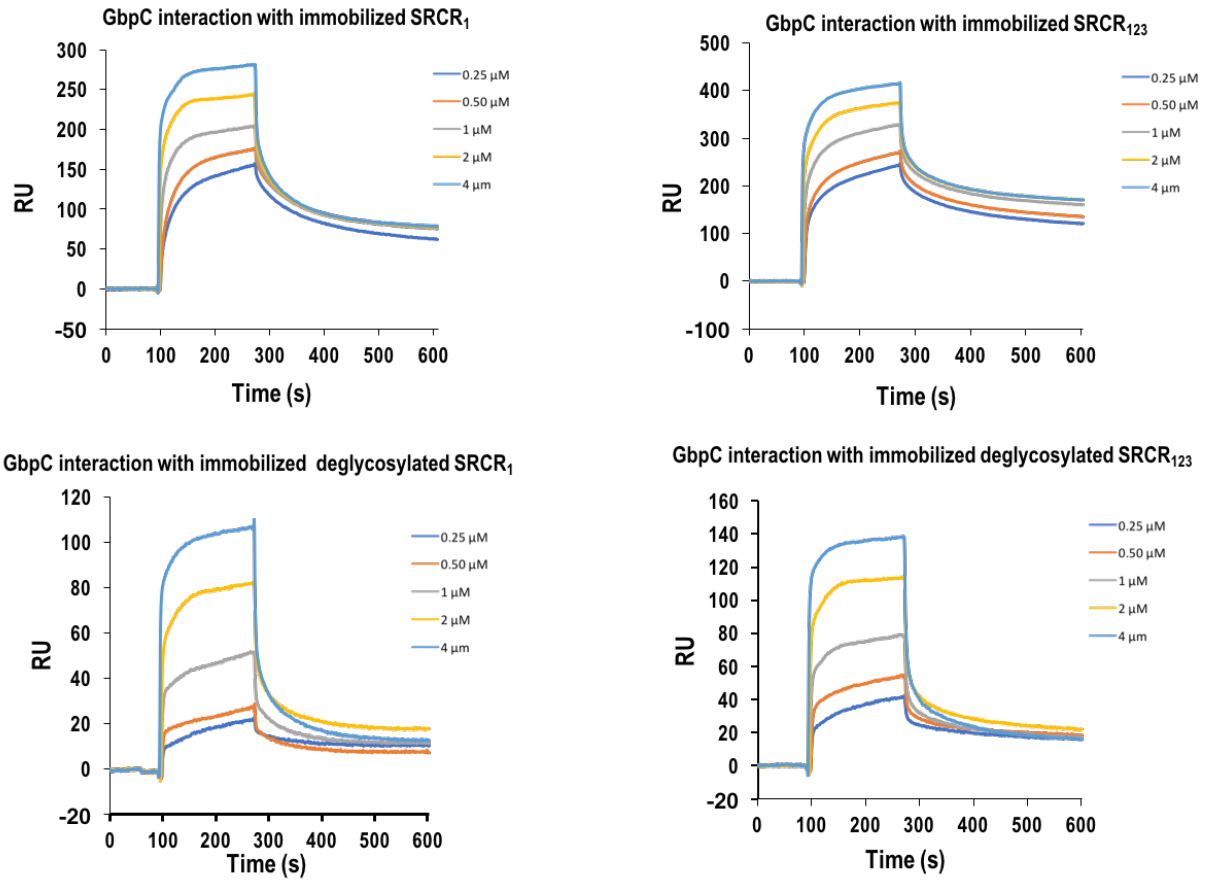

Supplemental Figure 9a: Panel shows SPR sensorgrams for the interaction between GbpC and SRCR, whose results are summarized in Table 2.

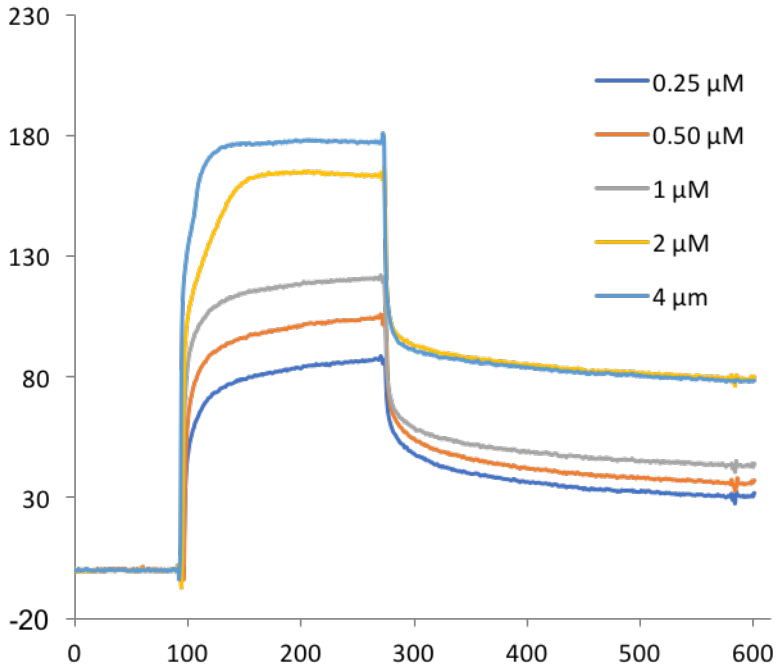

Supplemental Figure 9b: Panel shows SPR sensorgram for the interaction between GbpC and SAG, whose results are summarized in Table 2.

Affinities assessed from dextran inhibition experiments.				
Dextran (μM)	**GbpC (μM)**	**K_A (1/M)**	**K_D (M)**	**Chi^2**
0	4	4.43E+06	4.79E-06	1.48
	2	5.61E+06	1.82E-07	6.01
	1	1.00E+07	1.03E-07	1.79
40	4	5.38E+06	1.92E-07	4.96
	2	7.11E+06	1.42E-07	3.02
	1	1.24E+07	8.43E-08	1.15
80	4	3.32E+06	1.44E-06	2.17
	2	4.90E+06	2.05E-07	2.14
	1	9.91E+06	1.04E-07	0.65
160	4	4.03E+06	2.55E-07	3.12
	2	5.17E+06	6.86E-06	1.60
	1	3.58E+06	2.80E-07	0.50

Supplemental Table 1: Table describes the observed affinities in the dextran inhibition experiment, in which the adherence of GbpC to immobilized SRCR was analyzed. While we observe that the amount of protein bound on the chip surface decreases in a dose dependent manner, their affinities remain unchanged in the presence of dextran. This indicates the possibility of steric hindrances brought by dextran that would preclude the adherence of GbpC to SRCR.

	B-factor (Å^2) for residues loop region 410-418									Average
	V410	**N411**	**A412**	**D413**	**G414**	**T415**	**P416**	**R417**	**A418**	
Native	26.7	34.5	34.5	41.3	37.5	40.2	35.0	35.3	17.2	33.6
BGC-complex	32.7	45.7	49.6	56.2	48.4	44.0	39.6	45.6	27.5	43.3
GbpC Native (for the whole protein)										18.2
Gbpc + BGC (for the whole protein)										20.7

Supplemental Table 2: The table describes the observed B-factor values for the loop region 410-418 of GbpC in both the native and the complex structure. The B-factor values are higher for these loop regions compared to the average values for the native and the complex structure. This indicates that this region is highly flexible, and could shift to accommodate the ligand.